Motion of Spherical Particles After Impinging on a Flat Plate

Kim, Byung Moon
Institute of Advanced Material Study, Kyushu University

Aramaki, Shinichiro
Institute of Advanced Material Study, Kyushu University

https://doi.org/10.15017/7903

出版情報：九州大学機能物質科学研究所報告. 13 (1), pp.1-5, 1999-07-08. 九州大学機能物質科学研究所
バージョン：
権利関係：

Motion of Spherical Particles After Impinging on a Flat Plate

Byung Moon KIM and Shinichiro ARAMAKI

The visualization and the calculation of particle trajectory impinging on a flat plate are investigated by using Ar^+ laser, a camera and an equation of particle motion simplified by the terms of inertia force, drag, gravitational force and lift. The jet velocity was 6.9 m/s and 15 m/s. The spherical glass beads of 30, 58 and 100 μm in diameter were used. The distance between the nozzle exit and the plate was ten times the nozzle diameter. The photographs of particle motion that trajectory show that one is the first-impingement and rebound, which depends on the momentum of particle; and the other is the second-impingement, which depends on the particle diameter and the entrainment velocity of environment air. The maximum rebound height of particle increases with the particle diameter. Magnus effect appears in the particle trajectory over - 6000 rad/s in angular velocity.

Introduction

A motion of impinging particle is found in natural field as a pollutant material flow and in the following engineering cases; a cascade impactor, a surface treatment, a heat transfer promotion, a plasma jet coating (Suryanarayanan R) [1], a clean-room environment and various internal combustion engines. Impinging particle is widely applied in an engineering field because it is relatively easy to control the velocity and a number density of particles, and it can improve the heat transfer in a local region. A few of studies have been made for investigating a mechanism of heat transfer and a motion of impinging particle. Yoshida et al. [2] experimentally investigated a mechanism of heat transfer of a two-dimensional impinging jet with glass beads using a laser-doppler anemometry. They explained that the enhanced heat transfer around the stagnation point was attributed to the drastic change in the turbulent structure caused by relative motion between the rebound particles and air. Shimizu et al. [3] and Kurosaki et al. [4] investigated a heat transfer efficiency for particle size, impinging distance, and loading ratio. They expected that the reason of the heat transfer increase were a direct heat exchange between impinging particle and plate (Shimizu et al.) and disruption of the viscous sublayer (Kurosaki et al.) near the stagnation region. Most of the above studies for the particle motion and the increased heat transfer are focused mainly on the stagnation region. However, qualitative data for particles trajectory impinging on a plate has not been obtained. Anderson et al. [5] experimentally investigated the mutual relationship between particle and vortex in the stagnation region. They found that the radial velocity of particles gradually increased after reaching the peaks of their rebound trajectories where their residence times were longest. They also found that the radial velocity of fluid increased as approaching to the plate, but radial acceleration of large particles was impeded by both the large mass and the low fluid radial velocities which encountered during rebound, and the influence of vortices on velocities in the stagnation zone was limited only to the region close to the shear layer.

The purpose of the present work is to obtain a qualitative understanding of the impinging particle on a flat plate. Particle trajectories are visualized using a laser sheet, and the particle trajectories after impingement are calculated based on an equation of particle motion for three various particle diameter (d_p= 30, 58 and 100 μm) and for two different jet velocities (u_j= 6.9, 15m/s).

Nomenclature

C_D = drag coefficient
d = nozzle diameter
d_p = particle diameter
$\bar{F}_E$ = force
$\bar{F}_L$ = lift
r = radial distance
u_b = rebound velocity at a plate
u_j = air velocity at nozzle exit
u_p = particle velocity
x = axial distance
ν = kinematic viscosity

Received April 20, 1999

ρ = density
ω = angular velocity

Experiment apparatus

The present experimental set-up of a nozzle, a flat plate, Ar^+ laser and a digital camera are shown in Fig. 1. The jet flow discharges into an ambient air through a circular pipe with diameter of 10 mm and length of 1000 mm. The particle trajectories, when the particle supply rate is 0.245 g/min with jet velocies 6.9 m/s and 15 m/s respectively, were photographically monitored. The Reynolds number based on the air velocity at nozzle exit and the nozzle diameter are 4500 and 9900, respectively. The coordinate system is defined as indicated in Fig. 1. Table 1 shows the particle velocities at nozzle exit measured by a PIV (particle image velocimetry).

The particle trajectories are observed based on a flow visualization technique using Ar^+ laser and a digital camera. The thickness of a light sheet is 3 mm. The digital camera (Minolta, RD-175) has three plate CCD, two of these detect the green signal, and the remaining one detects R/B. The image size is 1528x1146 pixels. The iris is 6.7 and the shutter speed is 1/2 s.

Table 1 Particle velocities at nozzle exit.

d_p(μ m)		30	58	100
u_j=6.9(m/s)	u_p (m/s)	5.88	5.16	4.50
u_j=15(m/s)		12.36	10.03	8.79

Equation of particle motion

To compare the calculated rebound height with the experimental results and to provide the detailed data for the rebound trajectory of particle diameters 30, 58 and 100 μm, the simplified equation of particle motion is used. Only the terms of force required to accelerate the particle, drag, gravitational force and lift affecting the motion of particle, are taken into consideration in the equation. Thus, the equation of particle motion can be simplified as Eq. (1),

$$\frac{\pi}{6} d_p{}^3 \rho_p \frac{d\vec{u}_p}{dt} = C_D \frac{\pi}{8} d_p{}^2 \rho_f \left|\vec{u}_f - \vec{u}_p\right| \left(\vec{u}_f - \vec{u}_p\right) + \vec{F}_E - \vec{F}_L \ , \quad (1)$$

where the $\vec{F}_E$ is the gravitational force and $\vec{F}_L$ is the lift force due to so called Magnus effect given as follow [6];

$$\vec{F}_L = \frac{\pi}{8} d_p{}^3 \rho_f \left(\vec{u}_p - \vec{u}_f\right) \times \vec{\omega} \ , \quad (2)$$

and C_D is drag coefficient given as follow [7];

$$C_D = \frac{24}{\left|\vec{u}_f - \vec{u}_p\right| d_p / \nu} + \frac{4}{\left(\left|\vec{u}_f - \vec{u}_p\right| d_p / \nu\right)^{1/3}} \quad (3)$$

Results and Discussion

Particle motion trajectory The observation of particle behaviors was separately made in three regions of the impinging jet; they are the impingement region, the rebound region and the wall jet region.

Figure 2 shows the particle trajectories for diameters 30, 58 and 100 μm in three regions with the jet velocies (6.9 m/s and 15 m/s). The particle exhibits a vertical motion toward the plate before the first-impingement. However, in the subsequent rebounding and the second-im-

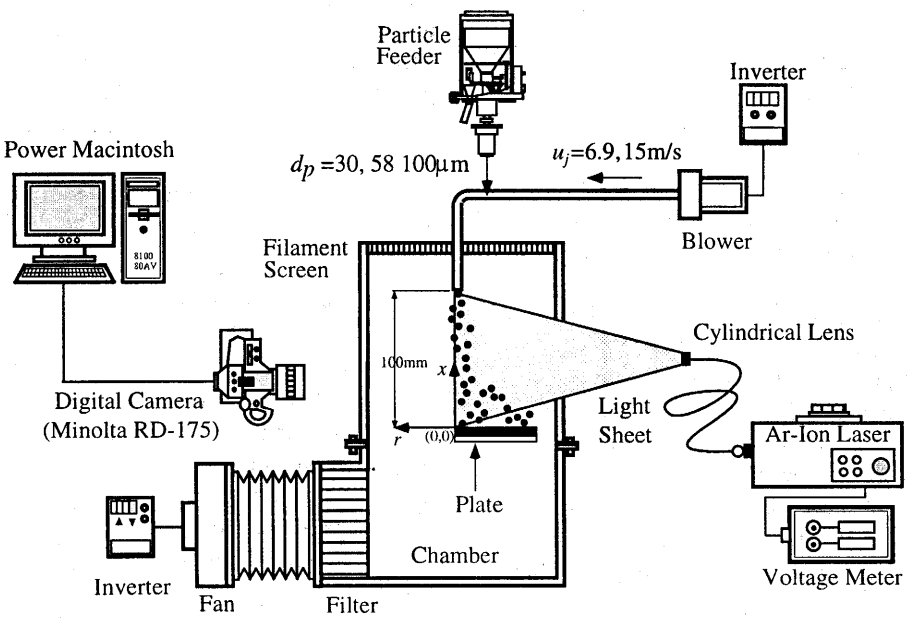

Fig. 1 Schematic diagram of experimental apparatus.

pinging stage, the trajectories of particles become parabolic.

As seen from Fig. 2 (a), for u_j=6.9 m/s, in the first-impinging stage, particles have impinged almost vertically to the plate. The particle motion in the wall jet region shows a sluggish parabolic trajectory due to air flow along the wall. For a case of u_j=6.9 m/s, and d_p=58 μm, the particle motion shows a sharp parabolic trajectories in the rebound region. For a case of u_j=6.9 m/s, and d_p=100 μm, a more sharp parabolic motion appears because of the in-

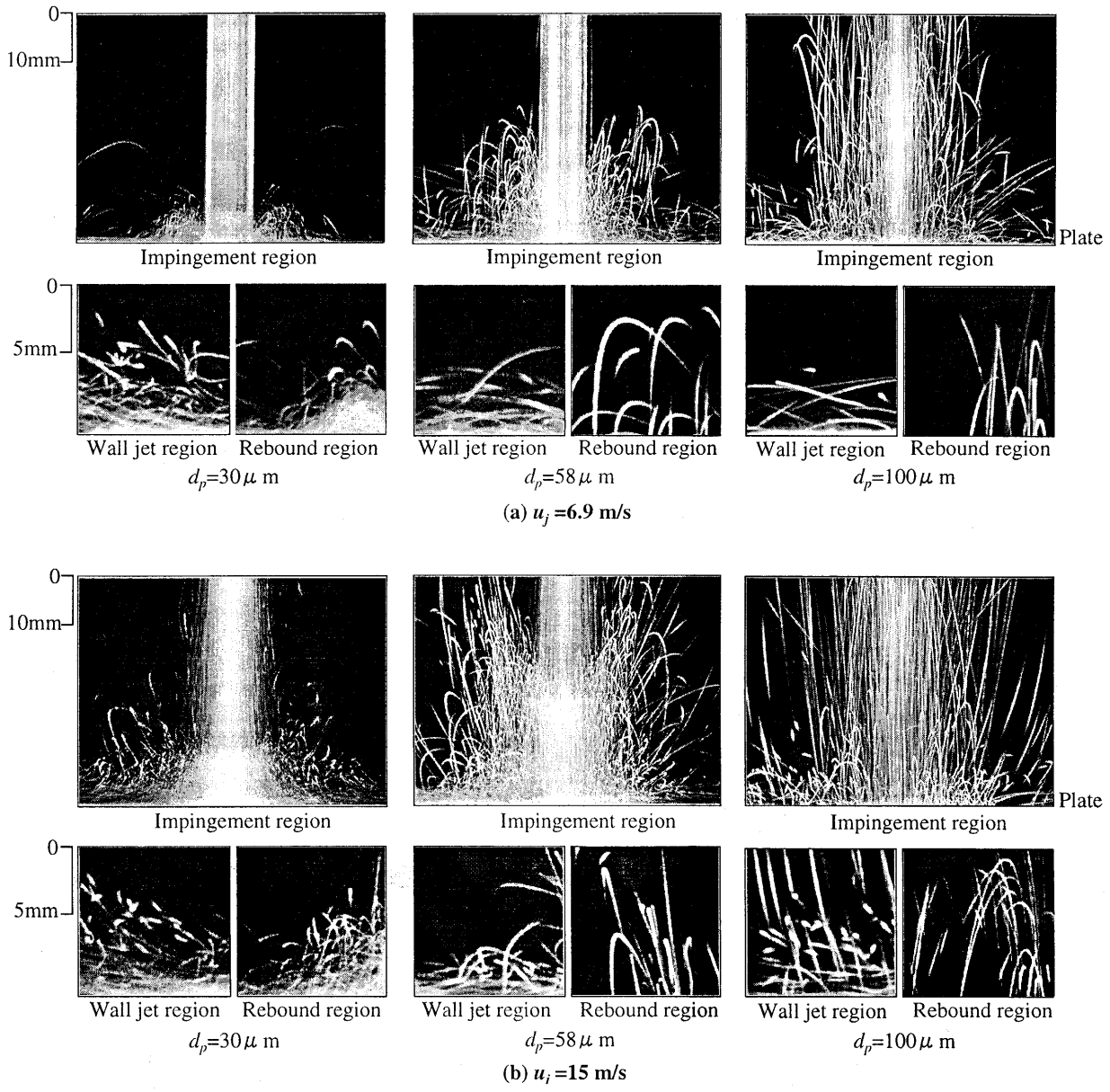

Fig. 2 The effect of particle size and jet velocity on particle trajectories impinging on a plate.

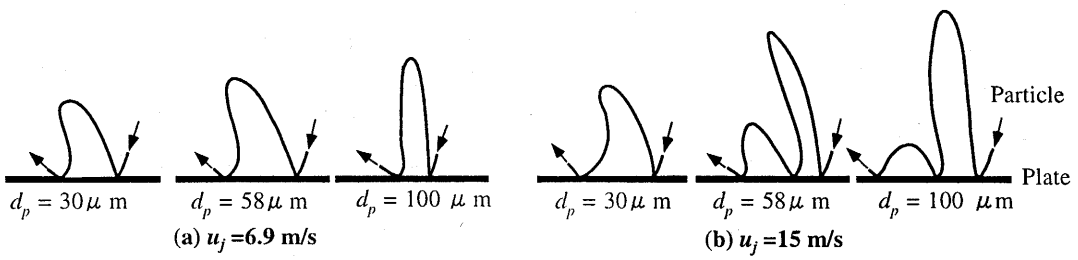

Fig. 3 Sketch of representative particle trajectories impinging on a plate.

crease in rebound height which caused by the increased momentum of particle. However, the particles in the wall jet region have a similar behavior.

For a case of u_j=15 m/s, and particle diameter 30 μm, spreading of particles at nozzle exit is observed as shown in Fig. 2 (b). This in turn caused the increase in impingement angle of the particles. The impingement angle begins to increase further due to wall jet. The rebound particles move toward the nozzle centerline due to entrainment velocity. Thus, the behaviors of particles are affected by the complicated air flow in the jet. For d_p=58 μm and u_j=15 m/s, the second-impinging particles move toward the nozzle centerline. However, the particles far from the impingement region fall vertically to the plate, because of less effect of the air entrainment. For u_j=15 m/s and d_p=100 μm, both the rebound height and the radius of curvature of the parabolic trajectory are greater than that for particle of 58 μm. But, the second-impingement is nearly vertical motion because it is not affected by the entrainment velocity. The particle motion in the wall jet region is very similar to that of diameter 58 μm.

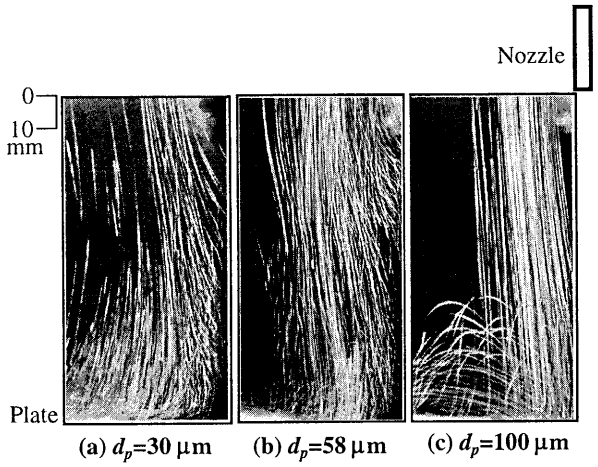

Fig. 4 Entrainment on particle trajectory with u_j =15 m/s.

The representative trajectories of particles impinging to the plate with different jet velocity are shown in Fig. 3. How larger the particle diameter is, how higher the rebound becomes. For the maximum rebound region, how larger the particle diameter and the jet velocity is, how heigher the maximum the rebound height becomes. The particles in about the plate move in a arc trajectory for the r-direction by air flow along the wall.

The effect of an entrainment velocity on particle motion with different particle diameter 30, 58 and 100 μm are shown in Fig. 4 by the free fall experiment of particle near nozzle for u_j=15 m/s. How smaller the particle diameter is, and how larger the incidence angle toward the jet centerline is, how more the particle move to the nozzle centerline.

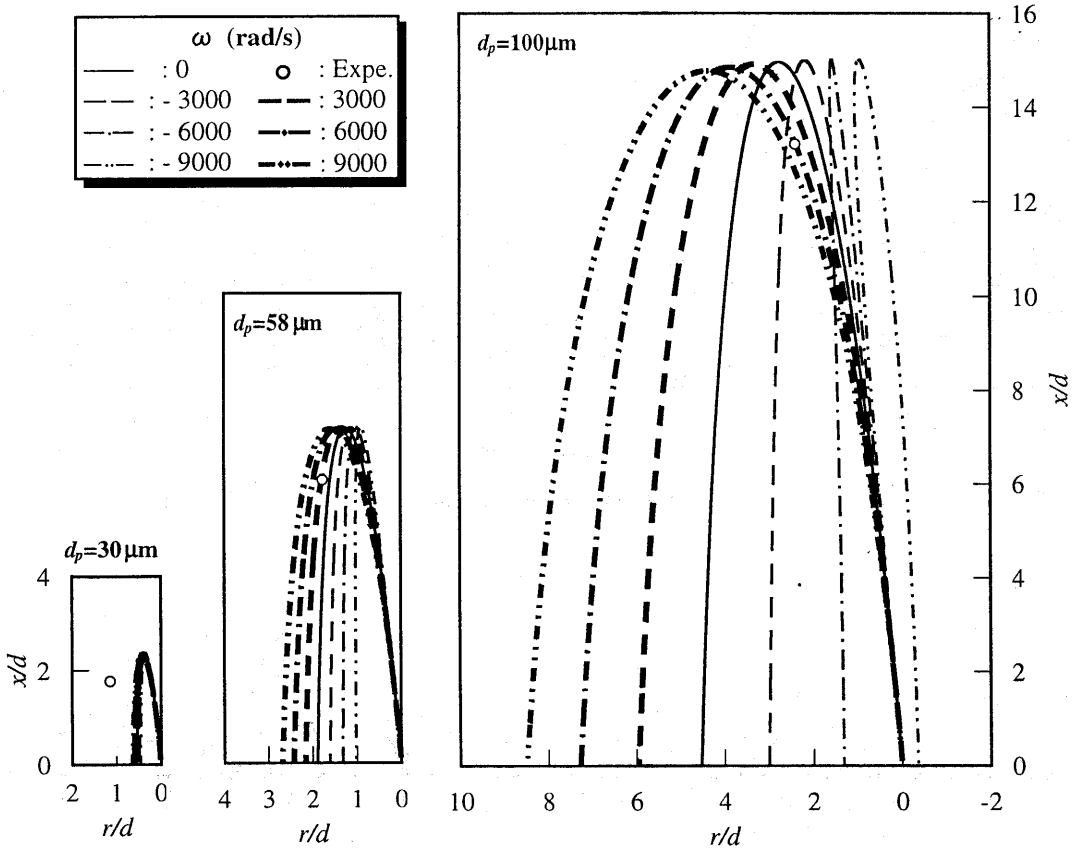

Fig. 5 Effect of particle angular velocity on particle motion trajectory, d_p=30, 58, 100 μm, u_j =15 m/s.

Motion trajectory of rebound particle The rebound trajectory of a single particle and the maximum rebound height are evaluated based on Eq. (1) and they are plotted in Fig. 5, where the height x and the radial distance r are normalized by the nozzle diameter d. In the calculation, the initial rebound velocity and the rebound angle at plate are used based on the experiment result as shown in table 2.

Table 2 Initial rebound velocity and angle at plate.

u_b(m/s)	Angle(deg)
9.8	5

The wall jet of fluid near a plate is ignored, the downflow velocity is assumed as -1.8 m/s in the calculation. Furthermore, it is assumed that the particle rotates around the axis perpendicular to x-r plate in the calculation.

In the figure the closed squares represent the experimental results, which correspond to the peak position of rebound particle trajectories. For $\omega = 0$ rad/s, a particle trajectory shows general parabolic motion. On the other hand, in the case of $\omega = -6000$ rad/s, the particle moves inward to the jet centerline. The result shows that the Magnus effect does not affect so much to the particle motion in the present case. The maximum rebound height of particle increases with the particle diameter.

Conclusion

The particle trajectory impinging on a flat plate was investigated by the flow visualization. The particle motion trajectory after impingement was calculated based on the conventional particle motion equation for particle diameters (30, 58 and 100 μm) and for the jet velocities (6.9 m/s and 15 m/s). From the results can be taken the conclusion as follow: From the observed particle trajectories in the three regions: the first impingement, the rebound and the second-impingement. The behaviors of particles in the second impingement region are influenced by the entrainment velocity of enviroment air. How smaller the particle diameter is, How larger the effect of entrainment velocity becomes. The effect of the entrainment velocity on the behaivors of particles is not so significant in the case of the particle with 100 μm in diameter. Magnus effect appears in the particle trajectory over -6000 rad/s in angular velocity. The maximum rebound height of particle increases with the particle diameter.

References

1. Suryanarayanan, R., Word Scientific Publishing Co. Pte. Ltd., (1933).
2. Yoshida, H., Suenaga, K., and Echigo, R., *Int.J. Heat Mass Transfer*,33–5 (1990), 859.
3. Shimizu, A., and Hasegawa, S., *Advances in Enhanced Heat Transfer, Proc. 18th National Heat transfer conf.*, San Diego, California, (1979), 155.
4. Kurosaki, Y., Murasaki, T., Satoh Y., and Kashiwagi, T., *Heat Transfer*, 5 (1986), 2587.
5. Anderson, S. L., and Longmire, E. K., *J.Fluid Mech.* 299 (1995), 333.
6. Rubinow, S. I., and Keller, J. B., *J. Fluid.* 11 (1966), 447.
7. Ueno, S., *master thesis of Kyushu university*, (1991), 250 (in Japanese).